

1 **Title:** Intermittent hormonal therapy shows similar outcome than SOC in ER+ breast  
2 cancer preclinical model.

3

4 **Authors:** Pedro M. Enriquez-Navas<sup>1</sup>, Libia Garcia<sup>1</sup>, Mahmoud Abdalah<sup>2</sup>, Olya  
5 Stringfield<sup>2</sup>, Kimberly Luddy<sup>1</sup>, Sabrina Hassan<sup>1</sup>, Robert J. Gillies<sup>1</sup>, and Robert A.  
6 Gatenby<sup>1</sup>.

7 **Affiliations:** (1) Department of Cancer Physiology and (2) Image Response Assessment  
8 Team (IRAT) Core, H. Lee Moffitt Cancer Center & Research Institute. 12902 Magnolia  
9 Dr. Tampa (FL) 33612.

10

11

## 12 **Corresponding Author**

13 Pedro M. Enriquez-Navas. [Pedro.enriqueznavas@mofitt.org](mailto:Pedro.enriqueznavas@mofitt.org). 813-745-1417.

14

15

16

17

18

19

20

21

22

23

24

25

26

27 **Abstract:**

28 Clinical breast cancers in which at least 10% of cells express the estrogen receptor are  
29 labeled as “ER positive.” First line therapy for these patients is typically continuous  
30 administration of anti-estrogen drugs at maximum tolerated dose (MTD) until  
31 progression. In the vast majority of patients, resistance to hormone therapy evolves in  
32 the breast cancer cells within 2 years leading to treatment failure and tumor  
33 progression. In prior studies, we have demonstrated continuous application of MTD  
34 chemotherapy results in evolutionary dynamics (termed “competitive release”) that  
35 accelerates proliferation of treatment-resistance populations. In contrast, evolution-  
36 informed application of treatment reduces drug administration to maintain substantial  
37 populations of therapy-sensitive cells to reduce proliferation of resistant phenotypes.  
38 Prior pre-clinical and clinical studies have shown this strategy can delay or prevent  
39 proliferation of resistant cells and prolong time to progression (TTP). We hypothesize  
40 that similar dynamics may be observed in hormonal therapy of ER+ breast cancers.  
41 Here we address two important dynamics. First, we consider a clinical scenario in which  
42 symptoms are sufficiently severe or life-threatening to require rapid and substantial  
43 tumor reduction. Can this be achieved while retaining evolutionary dynamics to  
44 subsequently delay proliferation of resistance? A second, related question is defining  
45 the cost of resistance to anti-estrogen therapy. Here, we investigated the evolutionary  
46 dynamics of resistance to anti-estrogen therapy using ER+ MCF-7 orthotopic  
47 xenografts treated with both continuous Tamoxifen as well as cycles in which estrogen  
48 stimulation is combined with estrogen suppression. As expected, continuous  
49 administration of anti-estrogen drugs successfully suppressed tumor growth. However

50 we found that brief interruptions in drug administration permitted equal tumor control  
51 while administering up to 50% less drug and maintaining cell phenotypes that retained  
52 high levels of ER expression and lower levels of MDR1 expression. In follow-on  
53 experiments combining hormonal and chemo-therapies; we obtained similar tumor  
54 control to hormonal therapy alone but with more necrosis and significantly lower ER  
55 expression in the surviving population.

56

## 57 **Introduction:**

58 In 2017 about 300,000 women in the United States were diagnosed with breast  
59 cancer and, among these, almost 90% were characterized as estrogen receptor positive  
60 (ER+) [1, 2]. The criteria for ER+ requires that at least 10% of the tumor cells express  
61 ER on immunohistochemical staining so that, in many breast cancers, a significant  
62 fraction of the cancer cells do not express ER and may be resistant to anti-estrogen  
63 therapy [3].

64 Initial treatment for ER+ breast cancer includes blockade of the effect of estrogen  
65 by selective estrogen receptor modulator (SERM) drugs.[4] Tamoxifen, which blocks  
66 the interaction between estrogen and its receptor impeding cell replication, is among the  
67 most widely used SERM drugs and is typically administered at maximum tolerated dose  
68 daily until tumor progression [5, 6]. Alternative strategies, such as aromatase inhibitors,  
69 block the synthesis of estrogen by normal cells. While nearly all ER+ tumors initially  
70 respond to anti-estrogen therapy, evolution of resistance with treatment failure and  
71 tumor progression typically is observed within a few months to a few years[7].

72           There are three major drawbacks in anti-estrogen treatment: (1) cost and side  
73 effects reduce compliance in up to 25% of the patients [8]; (2) about 10% will develop  
74 one or more side-effects that require dose adjustments or treatment cessation [1, 7, 9];  
75 (3) prolonged continuous treatment may significantly increase risk for endometrial  
76 cancer. Nevertheless, the vast majority of patients initially respond to anti-estrogen  
77 therapy but development of resistance leading to treatment failure and progression is  
78 virtually inevitable [10-12] and, among the multiple mechanisms of resistance, evolution  
79 of estrogen-independent growth is most common[11].

80           A common evolution-based strategy to delay tumor progression focuses on the  
81 phenotypic cost of resistance. This is readily apparent in resistance to chemotherapy  
82 based on increased expression of MDR1 (Multi-Drug Resistance system-1); a  
83 membrane glycoprotein (PgP) that is an active ATPase pump extruding lipophilic  
84 cationic xenobiotics. In some studies, up to 40% of a cell's energy budget must be used  
85 to synthesize, maintain, and operate MDR membrane pumps – an obvious cost of  
86 resistance [13, 14]. Thus, a strategy termed “adaptive therapy” explicitly limits cancer  
87 treatment to maintain a significant population of treatment-sensitive cells. Therapy is  
88 then withdrawn. However, in the subsequent tumor regrowth, the sensitive cells, in the  
89 absence of the cost of resistance, outcompete the resistant cells. Thus, through multiple  
90 cycles, the tumor population remains sensitive to the primary treatment. In an ongoing  
91 clinical trial in metastatic castrate-resistant prostate cancer, we have found that  
92 treatment that only reduces the serum PSA to half of its pre-treatment value can both  
93 substantially increase the time to progression while decreasing the cumulative drug  
94 does [15].

95           A number of questions regarding optimal evolution-based treatments remain.  
96   Among these, perhaps the most urgent is the apparently conflicting demands for  
97   treatment in which a patient presents with highly symptomatic or potentially life-  
98   threatening conditions. Here, rapid and significant reduction of the tumor burden is  
99   clinically necessary but could also result in competitive release of resistant clones that  
100   result in rapid proliferation leading to tumor failure and tumor progression with recurrent  
101   symptoms. Here we examine potential treatment strategies that can both rapidly  
102   diminish tumor burden to very low levels while maintaining evolutionary dynamics that  
103   can prolong tumor control and reduce the cumulative drug dose to reduce toxicity and  
104   cost.

105           A second question in this study is the cost of resistance to hormonal therapy.  
106   Although drug efflux by the MDR proteins is a mechanism of resistance in ER+ cells,  
107   clinical studies have found that, in general, durable resistance to estrogen therapy is  
108   most commonly obtained in breast cancer cells through expression of alternative  
109   pathways that permit estrogen-independent survival and proliferation. However, unlike  
110   the dynamics of PgP, the evolutionary cost of estrogen-independence is not obvious.  
111   Nevertheless, that such a cost exists can be inferred using a concept termed  
112   “evolutionary triage.” Briefly, “evolutionary triage”[15] simply states that, among  
113   competing populations, the fittest phenotype will be the most proliferative and, in  
114   general, be the largest population. Therefore, in general, the relative fitness of each  
115   cancer subpopulation can be estimated by their relative abundance within the tumor.  
116   This, however, yields puzzling results for ER+ breast cancers in which greater than 50%  
117   of the cells do not express the ER on immunohistochemical stains. Despite ER+ cells

118 being in the minority, these tumors still typically respond, at least initially, to anti-  
119 estrogen therapy suggesting some component of the treatment dynamics is not being  
120 captured in the IHC results. Thus, it is not clear if evolution-based treatment strategies  
121 could be successfully applied in clinical treatment of ER+ metastatic breast cancer.

122 Here, we address these questions in pre-clinical studies. Our results showed that  
123 (i) intermittent therapies can control tumor growth with less Tamoxifen (using as little as  
124 50% of the standard dose), (ii) the ER expression is maintained at or above the levels of  
125 SOC, (iii) expression of MDR1 was reduced in tumors treated with intermittent  
126 tamoxifen therapy, and (iv) the combination of hormonal- and chemo- therapies in the  
127 presence of high levels of estrogen kept the tumor at the same volume than the  
128 standard therapy, although showing more tumor necrosis.

129 We conclude that evolution-based administration of anti-estrogen drugs in  
130 patients is likely to benefit patients with metastatic ER+ breast cancer compared to  
131 current strategies of continuous MTD dosing until progression. Our results, however,  
132 also suggest the evolutionary dynamics that govern estrogen-related fitness in breast  
133 cancer cells and the clinical efficacy of anti-estrogen therapy are not fully understood  
134 and require further investigation.

135

## 136 **Materials and Methods**

### 137 *In-vivo Experiments*

138 Different cohorts (n= 10, 14, 4, and 39) of nude (nu/nu) mice were injected in the  
139 mammary fat pad with  $5 \times 10^6$  MCF7 cells (injected in a mixture 1:1 with phenol-red free  
140 Matrigel) tagged with GFP (cells were obtained from ATCC, and were grown following

141 its guidelines, cell culture media and supplies were obtained from Thermo Fisher  
142 Scientific). Prior to the cell injections, an estrogen pellet (Innovative Research of  
143 America) of 0.72 mg of  $\beta$ -estrogen with 90 days slow release was subcutaneously  
144 implanted in each mouse, giving a continuous dose of 400 pg of estrogen per milliliter of  
145 blood. If the experiments lasted longer than 90 days, a similar pellet was implanted to  
146 the mice.

147         When tumors reached 300 mm<sup>3</sup> approximately, mice were randomly distributed  
148 in groups and treated following one of the subsequent treatments: *Controls* (Ctrl), no  
149 treatment; *Tamoxifen standard* (TamST), 0.5 mg of tamoxifen per mouse daily;  
150 *Tamoxifen-vacation* (TamVac), 2 weeks of TamST followed by one week of no  
151 treatment (vacation); *Tamoxifen 2 weeks* (Tam2weeks), two weeks of TamST followed  
152 by 2 weeks of vacation; *Tamoxifen 3 weeks* (Tam3weeks), three weeks of TamST  
153 followed by three weeks of vacation; *Tamoxifen and Paclitaxel* (TamPac), 2 weeks of  
154 TamST followed by one week in which Paclitaxel is applied in two non-consecutive days  
155 at a concentration of 20mg/kg (ip) (PacST); *Vacation and Paclitaxel* (VacPac), 2 weeks  
156 of no treatment followed by one week in which 20 mg/kg of Paclitaxel in applied in two  
157 non-consecutive days; *Paclitaxel and Tamoxifen* (PacTam), one week of PacST  
158 followed by two weeks of TamST.

159         Tamoxifen (Caiman Chemical Company) was suspended in peanut oil (Sigma  
160 Aldrich) and given to animals by either i.p or gavage routes; initially Tamoxifen was  
161 administered in 200  $\mu$ l of peanut oil through i.p. injection. However, we changed the  
162 route of administration to gavage because mice were not able to metabolize the peanut  
163 oil and all of them died in a short period of time; maybe due to peritonitis (when tumors

164 were collected, we noticed that peanut oil was accumulated in mice abdomen).

165 Paclitaxel (LC laboratories) was dissolved in a mixture of Koliphor oil and ethanol (1:1,  
166 both solvents were obtained from Sigma Aldrich) and it was given via i.p. injection;  
167 before injection, the corresponding dose was diluted twice with PBS.

168 Mice were visually monitored, and their weights monitored once a week, to address any  
169 treatment toxicity issues. Tumor growth was measured once a week by either caliper,  
170 using the formula:  $vol = \frac{\pi}{6} * \frac{(short\ distance)^2}{long\ distance}$ , or by MRI; magnetic resonance data were  
171 acquired with a 7 T horizontal magnet Agilent ASR 310 (Agilent Technologies Inc.)  
172 equipped with nested 205/120/HDS gradient insert and a bore size of 310 mm. Before  
173 imaging, the animals were placed in an induction chamber and anesthetized with 2 -3%  
174 isoflurane delivered in 1.5 liter/min oxygen ventilation. After complete induction, animals  
175 were restrained in a custom-designed holder and inserted into the magnet while  
176 constantly receiving isoflurane (1 to 3%) within the same oxygen ventilation. Body  
177 temperature ( $37^{\circ} \pm 1^{\circ}\text{C}$ ) and respiratory functions were monitored continuously (SAll  
178 System) during the experimental time. A 35 mm Litzcage coil (Doty Scientific) was used  
179 to carry out axial T2-weighted fast spin-echo multislice experiments (acquired with  
180 TE/TR [echo time/repetition time] = 72 ms/1000 ms, field of view (FOV) =  $35 \times 35\text{ mm}^2$ ,  
181 matrix =  $128 \times 128$ , yielding a spatial in-plane resolution of 273  $\mu\text{m}$ , slice thickness of  
182 1.5 mm).

183 At the completion of the experiments (either tumor under control or when tumor  
184 volume reached  $\sim 2000\text{ mm}^3$ ) tumors were collected for histological analysis. After  
185 collection, tumors were processed for histological studies by soaking in formalin, during  
186 24 h at least, followed by embedding in paraffin blocks. Consecutive histological slices



187 (5  $\mu\text{m}$  thickness) were cut from each tumor to study the necrosis percentage (H&E),  
188 vascularity density and functionality (CD31 and SMA, respectively), estrogen receptor  
189 (ER) expression, and resistance mechanisms (by means of MDR1 expression). Once  
190 stained, the slices were imaged at the Moffitt Cancer Center microscope core facilities,  
191 using Aperio ScanScope XT microscope and Aperio Spectrum version 10.2.5.2352  
192 image analytic software (Leica Biosystems Inc.). To optimize the image analysis, we  
193 trained the analytic algorithm by using ROIs that were selected manually to represent  
194 ROIs that are positive or negative for each stain. After initial algorithm training, the  
195 software developed a final algorithm, which was used to automatically analyze the  
196 slides with a pixel-size resolution (5  $\mu\text{m}$  x 5  $\mu\text{m}$ ).

#### 197 *Imaging analysis*

198 To analyze the homogeneity in the ER expression, a radiomics analysis was  
199 performed on IHC estrogen receptor images. Features extraction was done on IHC  
200 digital images with the same magnification (x20). Color images were segmented using a  
201 thresholding method to identify the pixels that were positively stained. Pixels outside the  
202 segmented range (background and/or unstained cells) were discarded and not used for  
203 analyses. Masks from positively stained cells were used to generate neighborhood  
204 maps. For each pixel in the mask, the number of immediate neighbors that were also in  
205 the mask (positively stained) was counted (up to 8) and that number is the pixel's  
206 neighborhood coefficient. Thus, for all samples, the masks of positively stained pixels  
207 were replaced by corresponding neighborhood maps consisting of neighborhood  
208 coefficients. The neighborhood maps were computed to capture the distribution and the  
209 density of positively (ER+) stained pixels.

210           Following the generation of neighborhood maps, 202 2D image features were  
211   calculated from them, including statistical, shape, and texture variables. These features  
212   were then reduced by including only one feature from subsets of inter-correlated  
213   features (Pearson correlation coefficient > |0.8|). Among the final features list, only  
214   those features correlated with heterogeneity in the tissue texture were used to perform  
215   the analysis; table 1 shows a brief description of these features.

216   All the animal work during this project was done following the IACUC regulations of  
217   University of South Florida (Tampa) at the Moffitt Cancer Center facilities.

218           Statistical calculations were performed using the Excel software. Student's t-tests  
219   were performed considering two-tailed distribution and two samples with unequal  
220   variance.

## 221   **Results**

222           This project was designed to understand the evolutionary dynamics of resistance  
223   in ER+ breast tumors and, consequently, to improve first-line treatment of estrogen  
224   receptor positive (ER+) breast cancers with SERMs, such as Tamoxifen.

225   Treatment algorithms used in this study were suggested by preliminary *in-vitro* data in  
226   which MCF7 cells were grown under different microenvironment conditions to study the  
227   expression of the estrogen receptor following addition of Tamoxifen and/or Paclitaxel  
228   media.

229           In the first cohort of mice (n = 10) bearing orthotopic MCF7 tumors, Tamoxifen  
230   treatment was administered by i.p. injections. As it is shown in **Figure 1A**, treatment  
231   algorithm with a one-week vacation (TamVac) maintained tumors at similar volumes as  
232   standard treatment (TamST). No increase in tumor volume was observed during the

233 vacation period. Furthermore, at completion of the study, the remaining tumor cells  
234 demonstrated greater ER expression compared to the control and equal or greater  
235 expression the continuous dose cohort (**Figure 2A**).

236 TamST treatment achieved the same level of control as continuous high dose  
237 tamoxifen. This is in contrast to prior reports in which this combination was  
238 unsuccessful. [16-18]. It is possible this difference is due to treatment schedule. We  
239 treated the animals 7 days per week (matching the daily dose used clinically) and it  
240 appears that in the prior studies treatment was not administered on weekends. While  
241 the results were encouraging, we noted that all of the mice developed increased  
242 peritoneal fluid that appeared to be caused by the peanut oil used in the Tamoxifen  
243 injections.

244 In a second cohort (n=14) we used higher concentration of Tamoxifen (50 mg/ml)  
245 with 20  $\mu$ l of the suspension injected i.p. daily. This reduced the peritoneal fluid  
246 collection and showed the same outcome as the prior cohort (**Figure 1B**).

247 Histological analysis of ER expression showed no significant difference between the  
248 intermittent and standard tamoxifen therapies (**Figure 2B**). However, the vascularity  
249 (density and functionality) was decreased in TamVac therapy (**Figure 3**, columns A and  
250 B). MDR1 was expressed in the Tamoxifen therapy groups suggesting membrane  
251 extrusion play a significant role in evolution of resistance in this setting (**Figure 4B**).

252 Finally, because the ip injection of Tamoxifen was associated with peritoneal lipid  
253 collections, we examined an additional cohort of mice (n=41) in which Tamoxifen was  
254 administered by gavage (no significant difference was found between ip and gavage  
255 treatments, **Sup. Figure 1**). This cohort included prior treatment (continuous Tamoxifen

256 dosing and one-week vacation period) but also examined longer “vacation” periods  
257 during which treatment was suspended for 2 or 3 weeks (Tam2weeks and Tam3weeks).  
258 We also examined alternative sequences with Tamoxifen first followed by Paclitaxel or  
259 vice-versa (TamPac and PacTam, respectively).

260         After 130 days of treatment, no significant differences in tumor control were  
261 noted in the groups (**Figure 1C**). However, TamVac, Tam2weeks, and Tam3weeks  
262 groups had a cumulative dose reduction of 33, 50, and 50%, respectively. No  
263 significant tumor growth during these vacation periods was noted (**Figure 1** (grey zones  
264 represents vacations periods)). At necropsy, the tumors treated with vacation periods  
265 had slightly higher expression of estrogen receptor compared to continuous Tamoxifen  
266 (**Figure 2C and Sup. Figure 2**). Interestingly, vessel density and functionality were  
267 increased in tumors in which hormonal therapy was combined with a cytotoxic drug  
268 (**Figure 3**) but these tumors also demonstrated relatively larger fractions of necrosis  
269 (**Figure 3 and Sup. Figure 3**) when compared to the other cohorts.

270 We studied the expression of MDR1 systems for cohorts B and C using  
271 immunohistochemistry (IHC) (**Figure 4**). In general, cohorts with vacation periods  
272 showed lower expression of MDR1 than the continuous Tamoxifen group (**Figure 4, B**  
273 and C) reflecting the diminished selection pressure for resistance during treatment  
274 vacation.

275         We analyzed the homogeneity in the ER expression in the treatment cohorts  
276 using a “neighborhood” imaging analysis, which examined variations in ER expression  
277 in physically adjacent cell groups. To do so, we created a mask for the tumor slices  
278 following IHC staining for ER expression. An algorithm calculates probability that each

279 ER+ pixels will have similar adjacent pixels (up to 8). This analysis found increased  
280 numbers of ER+ similar “neighbors” in treated tumors with either Tamoxifen SOC or  
281 intermittent therapies compared to tumors also treated with chemotherapy (**Figure 5**).

## 282 **Discussion**

283 Cancer cells, like all living systems, evolve to adapt to local environmental  
284 selection forces. When clinical therapy is applied, evolution of resistance is commonly  
285 observed leading to treatment failure and tumor progression. Here we examine the  
286 evolutionary dynamics of ER+ breast cancer treated with anti-estrogen therapy, the  
287 typical first line clinical treatment for ER+ breast cancers. In prior pre-clinical and  
288 theoretical studies we have found that continuous application of therapy at MTD  
289 maximally selects for resistance – a well-known phenomenon in pest management  
290 termed “competitive release.” By periodically withdrawing therapy, we reduced the  
291 environmental selection forces for resistance by permitting survival of some treatment-  
292 sensitive cells. In the absence of treatment, the fitness advantage of the sensitive cells  
293 tended to suppress proliferation of the resistant phenotype thus prolonging tumor  
294 response. Here we addressed two potential barriers for applying this strategy to ER+  
295 clinical breast cancers. First, in patients who are symptomatic, optimal therapy must  
296 reduce the tumor burden below some symptomatic threshold before it is withdrawn.  
297 Second, we were concerned with the possibility that the tumor might rapidly progress  
298 after treatment withdrawal leading to rapid loss of control and thus decreased TTP.

299 In these pre-clinical experiments with ER+ breast cancers, we demonstrated  
300 intermittent application anti-estrogen drugs could achieve complete tumor control  
301 identical to that obtained with continuous MTD treatment. No tumor growth was

302 observed even during a 3-week interval during which therapy was not applied.  
303 Advantages of this therapy included a significant (up to 50%) cumulative dose reduction  
304 and decreased evidence tumor cell resistance (based on ER and MDR1 expression).  
305 Our study does not demonstrate that Tamoxifen intermittent therapy can prolong  
306 response as it we have found in chemotherapy for breast cancer in pre-clinical studies  
307 and hormone therapy in prostate cancer. Here we were primarily focused on  
308 experiments that address a clinical scenario in which the patient presents with highly  
309 symptomatic or life-threatening disease requiring rapid and significant reductions of the  
310 tumor burden. We demonstrate that such treatment can be administered to  
311 substantially reduce the tumor burden while also using interruptions of therapy to  
312 reduce evolutionary selection for resistant populations while still maintaining tumor  
313 control. Furthermore, these outcomes can be achieved while substantially reducing (by  
314 up to 50%) the total dose of Tamoxifen thus reducing toxicity and cost.

315 Finally, by imaging analysis (radiomics), we have demonstrated that  
316 evolutionary-based Tamoxifen therapies develop tumors with the same ER  
317 homogeneity than SOC. These results suggest that imaging biomarkers that correlate  
318 with intratumoral evolution during treatment may ultimately prove to be useful guides for  
319 evolution-based treatments.

320

321 **Acknowledgements:** This work has been supported in part by the SAIL Core, Tissue Core  
322 Facility, the Analytic Microscopy Core Facility, and by the IRAT Core Facility at the H. Lee  
323 Moffitt Cancer Center & Research Institute, an NCI designated Comprehensive Cancer Center  
324 (P30-CA076292).

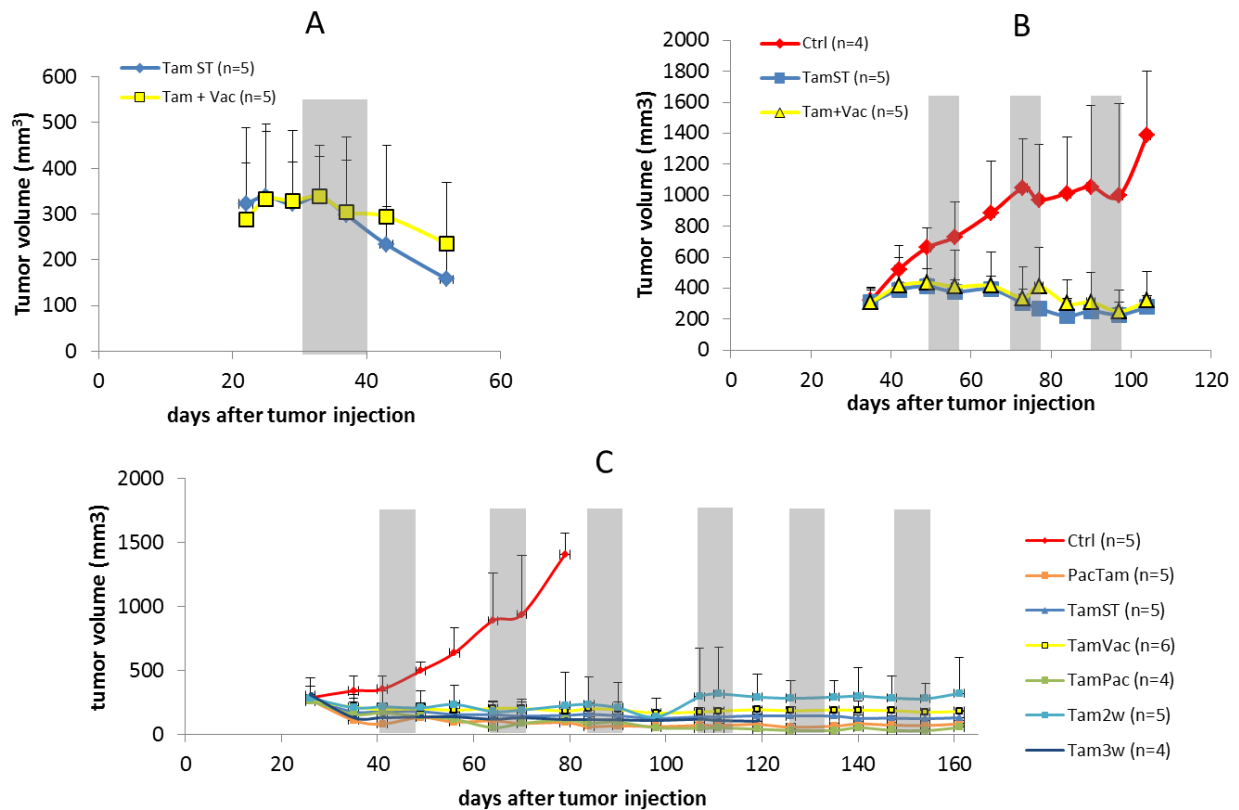
325 **References:**

- 326 1. <http://www.breastcancer.org/>. 2016.  
327 2. ACS, [www.cancer.org](http://www.cancer.org). 2016.  
328 3. Viale, G., *The current state of breast cancer classification*. Ann Oncol, 2012. **23 Suppl 10**: p. x207-  
329 10.  
330 4. Lumachi, F., et al., *Treatment of estrogen receptor-positive breast cancer*. Curr Med Chem, 2013.  
331 **20**(5): p. 596-604.  
332 5. Burstein, H.J., et al., *Adjuvant endocrine therapy for women with hormone receptor-positive*  
333 *breast cancer: american society of clinical oncology clinical practice guideline focused update*. J  
334 Clin Oncol, 2014. **32**(21): p. 2255-69.  
335 6. Lumachi, F., D.A. Santeufemia, and S.M. Basso, *Current medical treatment of estrogen receptor-*  
336 *positive breast cancer*. World J Biol Chem, 2015. **6**(3): p. 231-9.  
337 7. Shapiro, C.L. and A. Recht, *Side effects of adjuvant treatment of breast cancer*. N Engl J Med,  
338 2001. **344**(26): p. 1997-2008.  
339 8. Partridge, A.H., et al., *Nonadherence to adjuvant tamoxifen therapy in women with primary*  
340 *breast cancer*. J Clin Oncol, 2003. **21**(4): p. 602-6.  
341 9. [www.cancerresearchuk.org](http://www.cancerresearchuk.org). Tamoxifen. 2016.  
342 10. Colleoni, M., et al., *Annual Hazard Rates of Recurrence for Breast Cancer During 24 Years of*  
343 *Follow-Up: Results From the International Breast Cancer Study Group Trials I to V*. J Clin Oncol,  
344 2016. **34**(9): p. 927-35.  
345 11. Chang, M., *Tamoxifen Resistance in Breast Cancer*. Biomolecules & Therapeutics, 2012. **20**(3): p.  
346 256-267.  
347 12. Hayes, E.L. and J.S. Lewis-Wambi, *Mechanisms of endocrine resistance in breast cancer: an*  
348 *overview of the proposed roles of noncoding RNA*. Breast Cancer Res, 2015. **17**: p. 40.  
349 13. Kam, Y., et al., *Sweat but no gain: Inhibiting proliferation of multidrug resistant cancer cells with*  
350 *"ersatzdroges"*. Int J Cancer, 2014.  
351 14. Silva, A.S., et al., *Evolutionary approaches to prolong progression-free survival in breast cancer*.  
352 Cancer Res, 2012. **72**(24): p. 6362-70.  
353 15. Zhang, J., et al., *Integrating evolutionary dynamics into treatment of metastatic castrate-*  
354 *resistant prostate cancer*. Nature Communications, 2017. **8**(1): p. 1816.  
355 16. Osborne, C.K., K. Hobbs, and G.M. Clark, *Effect of estrogens and antiestrogens on growth of*  
356 *human breast cancer cells in athymic nude mice*. Cancer Res, 1985. **45**(2): p. 584-90.  
357 17. Osborne, C.K., et al., *The importance of tamoxifen metabolism in tamoxifen-stimulated breast*  
358 *tumor growth*. Cancer Chemother Pharmacol, 1994. **34**(2): p. 89-95.  
359 18. Whitesell, L., et al., *HSP90 empowers evolution of resistance to hormonal therapy in human*  
360 *breast cancer models*. Proc Natl Acad Sci U S A, 2014. **111**(51): p. 18297-302.

361

362

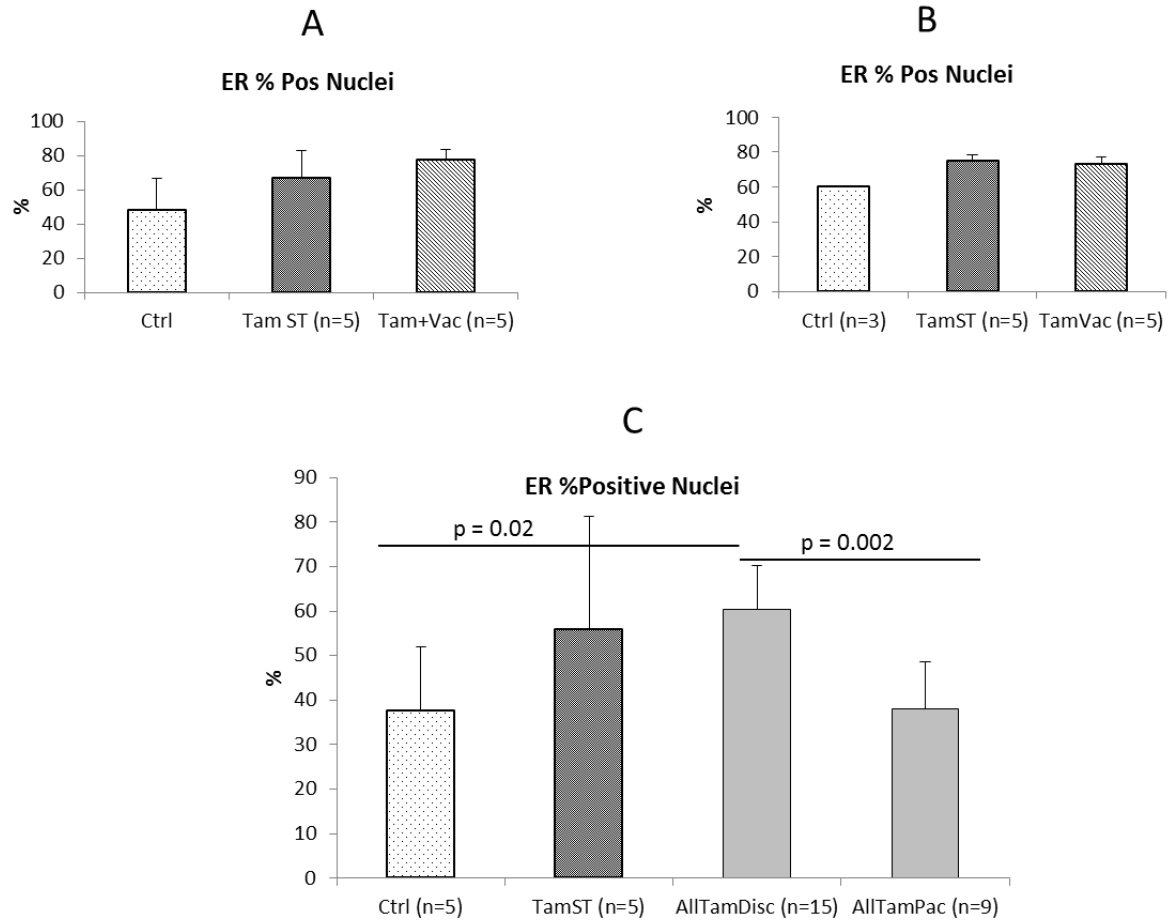
363 **Figures:**



364

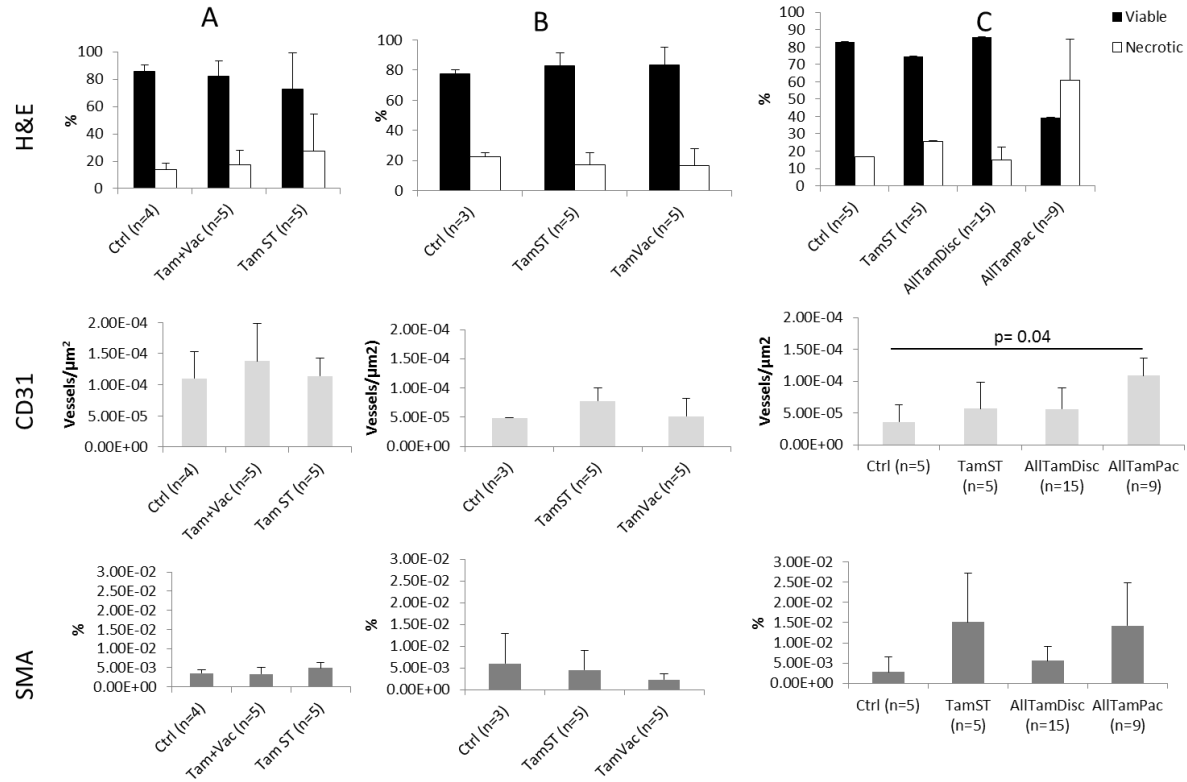
365 **Figure 1:** Tumor volumetric data of mice under different treatments. Grey zones  
366 correspond to either vacation periods or paclitaxel application (more information about  
367 each treatment can be found in Material and Methods section). Tumor volumes were  
368 measured by MRI. In parenthesis is the number of mice in each group. Data are shown  
369 by mean and error bars represent the standard deviation.





370

371 **Figure 2:** IHC analysis of the ER expression under different treatments. (Significance  
372 calculations were done by using a Student t-test with two-tailed distribution and  
373 considering two samples with unequal variance).

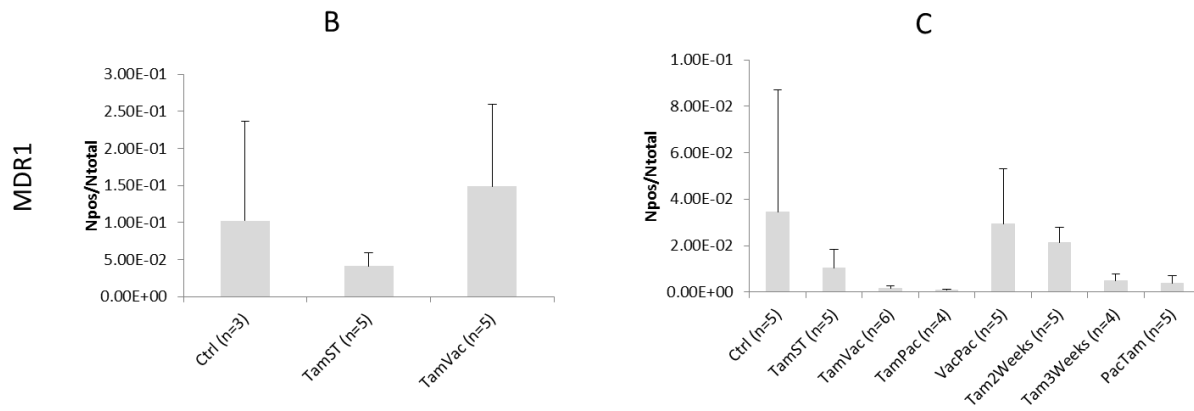


374

375 **Figure 3:** IHC analysis of viable and necrotic tissues (H&E), vessel density (CD31) and  
376 functionality (SMA) in tumors under different treatments. Data are shown by mean  
377 values with the standard deviation (error bars). p value calculated using Student t- test  
378 with two-tailed and unequal variance.

379

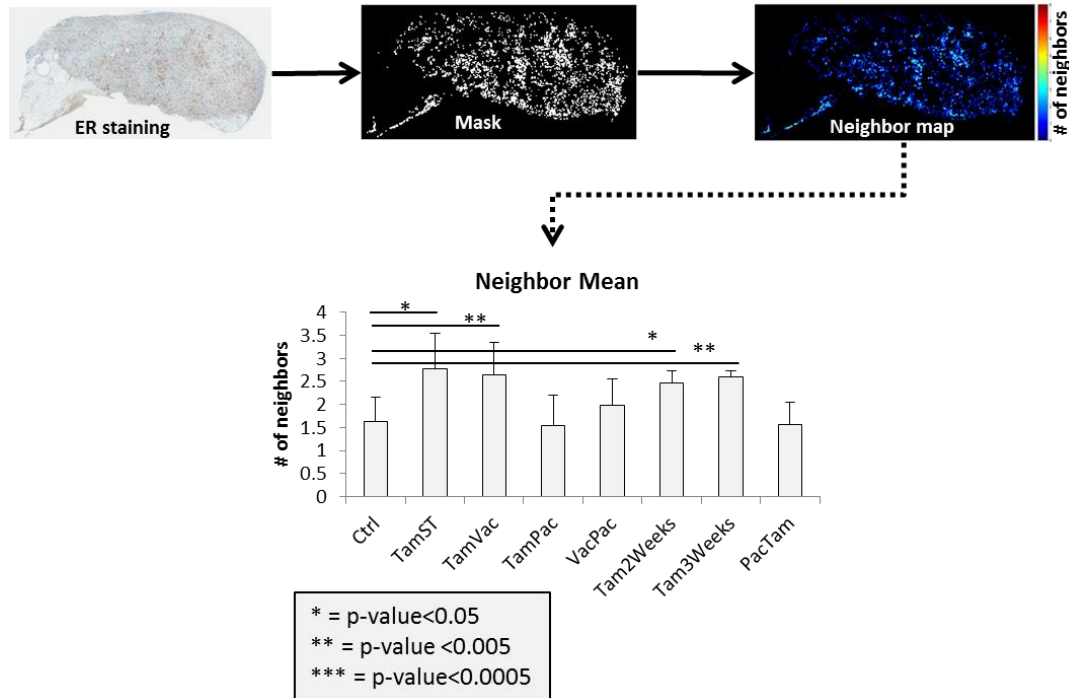
380



381

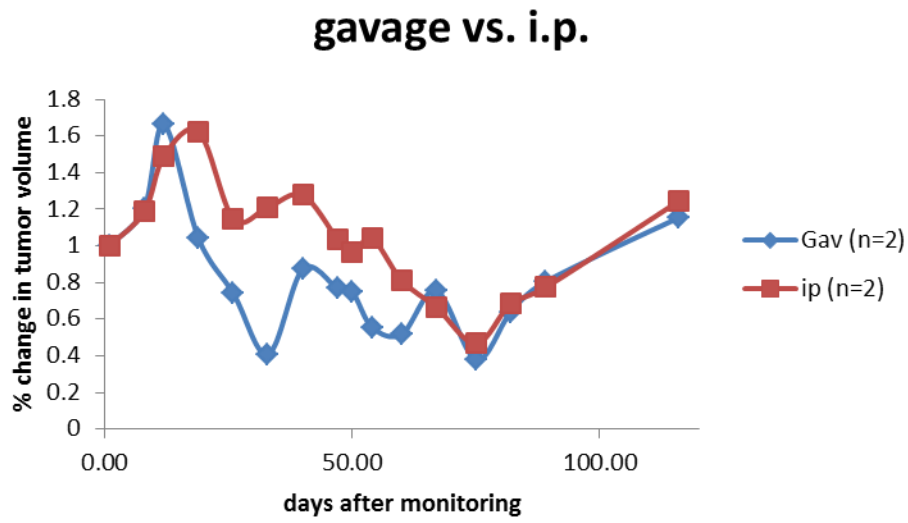
382 **Figure 4:** IHC analysis of the expression of MDR1 systems for cohorts B and C. Data is  
383 shown by mean with the standard deviation (error bars).

384



385

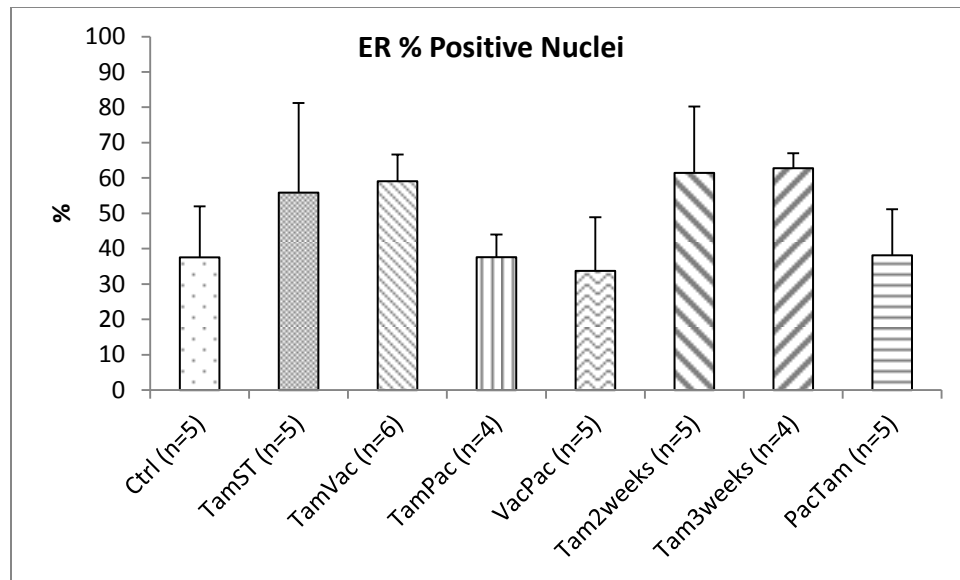
386 **Figure 5:** Radiomics analysis of ER expression. The neighbor map (ER+ pixels  
387 surrounded by similar ones) showing the mean value. Mean±SD is represented in bar  
388 graph. p-values are shown to compare the treated groups with the control (untreated)  
389 one.



390

391 **Sup. Figure 1:** Fold of change in tumor volume in mice treated with tamoxifen by either  
392 i.p. injections or gavage.

393



394

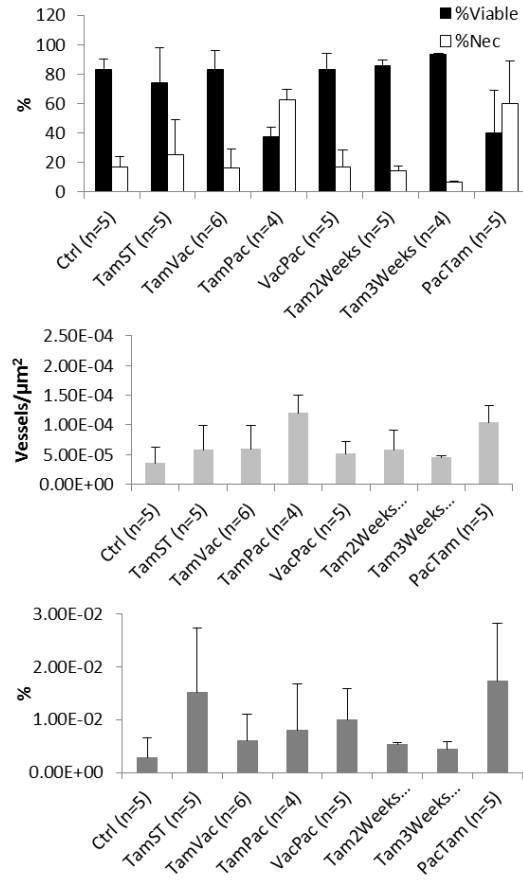
395 **Sup. Figure 3:** Cohort C IHC analysis of the ER expression under different treatments.

396 (Significance calculations were done by using a Student t-test with two-tailed distribution

397 and considering two samples with unequal variance).

398

399



400

401 **Sup. Figure 4:** Cohort C IHC analysis of viable and necrotic tissues (H&E), vessel  
402 density (CD31) and functionality (SMA) in tumors under different treatments.